

Effect of monomer hydrophilicity on ARGET-ATRP kinetics in aqueous mini-emulsion polymerization

Alicia Cintora | Florian Käfer  | Chenyun Yuan | Christopher K. Ober 

Materials Science and Engineering,
Cornell University, Ithaca, New
York, USA

Correspondence

Christopher K. Ober, Materials Science and Engineering, Cornell University, Ithaca, NY 14853, USA.
Email: c.ober@cornell.edu

Funding information

Air Force Office of Scientific Research, Grant/Award Number: FA9550-17-1-0038; NSF MRSEC Program, Division of Materials Research, Grant/Award Number: DMR-1719875; National Science Foundation, Grant/Award Number: DGE-1650441; Air Force Research Laboratory

Abstract

Activators regenerated by electron transfer (ARGET) atom transfer radical polymerization (ATRP)-based aqueous miniemulsion polymerization where the polymerization takes place in the stabilized monomer droplets is described. In this work, we compared styrene, *n*-butyl methacrylate (nBMA) and *tert*-butyl methacrylate (*t*BMA) and investigated the influence of their hydrophobicity on dispersity, molecular weight and particle stability based their partition coefficients ($\log P$) (2.67, 2.23, and 1.86, respectively). Tetrabutylammonium bromide (TBAB) was used as a phase transfer agent for the controlled delivery of Cu^{2+} -Br/tris(2-pyridylmethyl)amine (TPMA), a hydrophilic catalyst, into monomer droplets of varying hydrophobicity. The resulting dispersity and particle stability of each polymer is a function of its $\log P$ value, with the most hydrophobic monomer (styrene) displaying the narrowest dispersity and most control ($D < 1.3$), and the most hydrophilic polymer poly(*tert*-butyl methacrylate) (PtBMA) having reduced emulsion stability, determined by the observation of aggregate formation. Selected polymerization parameters, including effects of total ascorbic acid feed concentration and the monomer concentration and their effects on dispersity are reported. The controlled polymerizations of hydrophilic monomers using ARGET-ATRP in miniemulsion conditions and understanding the effect of monomer hydrophilicity on the emulsion stability will broaden the use of ARGET-ATRP in emulsion polymerization for the synthesis of polymer-grafted nanoparticles with hydrophilic corona.

KEY WORDS

ARGET-ATRP, hydrophilicity, mini-emulsion polymerization

1 | INTRODUCTION

Advances in aqueous dispersed phase polymerizations, including emulsion and miniemulsion reactions, have enabled control over molar mass and dispersity while becoming ever more environmentally benign by employing mild reactants and aqueous solvents. Additionally, these

particular systems provide facile transferability to industrial-sized scale-ups, as these polymerizations are typically effective at dissipating heat, making these methods especially attractive for commercial applications. Efforts to increase the eco-friendliness of these aqueous dispersed phase systems have also focused heavily on broadening the types of polymerization methods employed.

Various types of reversible-deactivation radical polymerizations (RDRPs) have been successfully applied to dispersed

Alicia Cintora and Florian Käfer contributed equally to this study.

phase polymerizations including reversible addition-fragmentation chain-transfer polymerization (RAFT),^{1,2} nitroxide-mediated radical polymerization (NMP),^{3–5} and atom transfer radical polymerization (ATRP).^{6–8} Particularly for ATRP, efforts to increase its commercial viability through the reduction of its air sensitivity and copper catalyst loading have formed a research area of high interest over the last two decades.^{9–15}

AGET ATRP has been the preferred method for miniemulsion polymerizations due to the facile oxidation of the Cu^{1+} catalyst to Cu^{2+} .^{16–20} Its extensive employment in heterogeneous systems allowed for a breadth of fundamental studies relating to control of molecular weights,¹⁸ colloidal stability,^{16,21} and later moved to development of more complex materials, such as gradient block copolymers and multilayered polymer particles.^{19,20,22} While AGET ATRP has been well studied and employed in the development of complex materials, the interest in further reducing metal catalyst loadings has enabled various ATRP systems to be developed such as ARGET,^{23–25} photomediated,^{26–28} and metal-free methods.^{29,30} Of those, only ARGET ATRP has been used in heterogeneous media.

Recent examples show that ARGET ATRP, which only employs ppm levels of catalyst, can be successfully used in miniemulsion systems. However, one of the biggest challenges in employing ARGET ATRP for heterogeneous polymerizations has been ligand selection. It is imperative that these ligands have the proper balance in their hydrophobicity: the ligand must be hydrophobic enough to enter the monomer droplets and at the same time, hydrophilic enough that it can effectively transport the catalyst through the aqueous phase. Efforts to design new ligands with these combined properties, have been extremely limited.²⁴ In consequence, methods with ppm levels (or less) of metal catalysts in heterogeneous media to develop complex polymer architectures have been limited.

On the other hand, highly active, yet, hydrophilic ligands, like tris(2-pyridylmethyl)amine (TPMA), have been considered incompatible with controlling polymerizations in heterogeneous media until recently. Such examples have taken advantage of ionic interactions between the ligand complex and a secondary component in the polymerization to drive such hydrophilic ligands into the monomer phase. Work by Wang et al.²³ successfully controlled the polymerization of acrylates and methacrylates using TPMA as the ligand by forming reactive ion-pairs between $\text{Cu}^{2+}\text{-Br/TPMA}$ and the anionic surfactant, sodium dodecyl sulfate (SDS). Recent work from our lab was able to control the polymerization of poly(methyl methacrylate) (PMMA) using TPMA as the ligand in an ARGET ATRP based *ab initio* emulsion polymerization using the nonionic surfactant, Pluronic F-127.²⁵ Instead of

deploying reactive ion pairs for effective transport between the aqueous phase and the monomer droplets, a halide salt, tetrabutylammonium bromide (TBAB), and the addition of acetone into the aqueous phase were used to aid phase transfer of the metal catalyst.

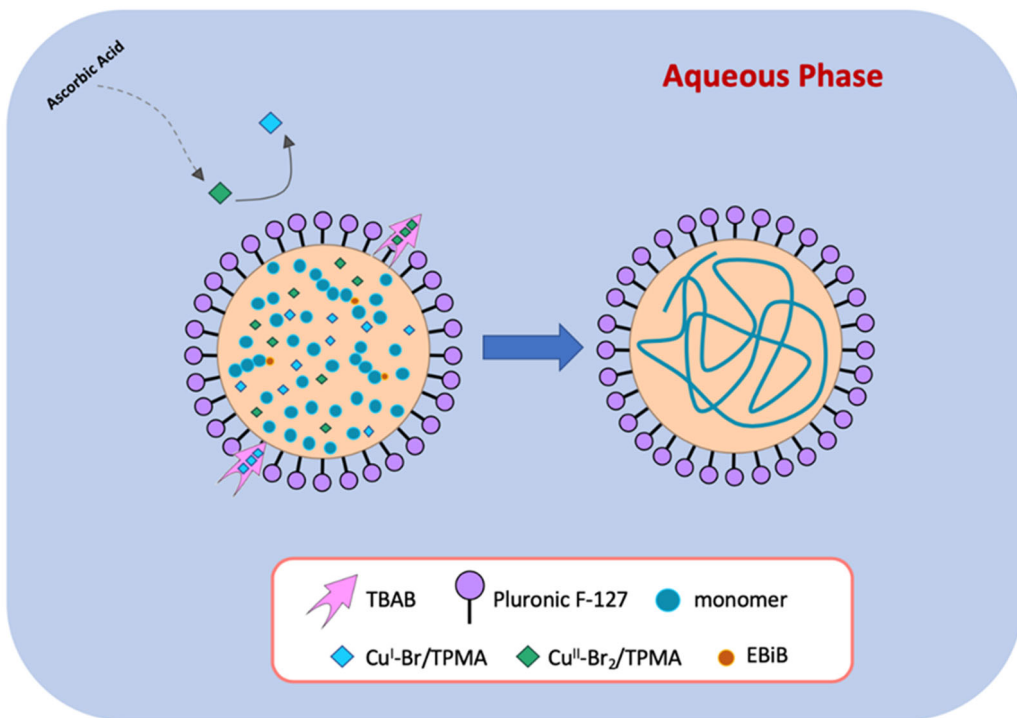
In this study, we expand on our previously reported ARGET ATRP-based system and here remove acetone from the aqueous phase to further reduce its environmental impact. Low dispersity of various monomers including styrene, n-butyl methacrylate (nBMA), and tert-butyl methacrylate (*t*BMA) was demonstrated in a controlled way without the aid of acetone. These modifications were shown to be capable of polymerizing hydrophobic monomers like styrene, with narrow dispersity (<1.3) and loadings as low as 0.149 $\mu\text{mol}/\text{ml}$ at various monomer concentrations to yield molar masses ranging 20–80 kg/mol. The hydrophobicity across all monomers was compared via their partition coefficients ($\log P$). It was concluded that reducing hydrophobicity of the monomer caused an increase in dispersity due to increased monomer diffusion between the organic/aqueous phase, reduced monomer/surfactant interactions and reduced polymer particle stability.

2 | RESULTS AND DISCUSSION

One of the benefits of using ARGET ATRP-based miniemulsion polymerizations is not only the high level of polymerization control but also its minimal environmental impact. Aqueous ARGET ATRP eliminates the need for toxic, high boiling point solvents and employs more benign reactants. However, our previous polymerizations of methyl methacrylate (MMA) relied on a 20 wt% acetone addition to the aqueous phase to enable movement of monomers and reactants between the aqueous and monomer phase, which produced polymers with very low dispersity.²⁵ Motivated by an interest in process simplification and to further reduce the environmental impact of this dispersed phase polymerization, we investigated the effect that removing acetone from the system plays in the synthesis of hydrophobic polymers. The reaction shown in Scheme 1 shows the polymerization process of our system. Ascorbic acid (AA) is slowly fed into the aqueous phase to reduce the inactive catalyst species $\text{Cu}^{2+}\text{-Br}_2\text{/TPMA}$ to its active form, $\text{Cu}^{1+}\text{-Br/TPMA}$.

Once the active catalyst species diffuses into the monomer droplets, the polymerization is initiated and propagates until the feeding of AA is stopped.

Additionally, previous reports from our group concluded that acetone was necessary for the solubility and transport of the active catalyst. However, herein we demonstrate that the polymerization approach can be applied to various monomers such as styrene, nBMA, and *t*BMA, resulting in narrow dispersity without the addition of



SCHEME 1 Mini-emulsion polymerization using ARGET-ATRP, feeding AA over time

TABLE 1 The effects of $[\text{AA}]:[\text{Cu}^{2+}]$ ratio on polymerization molecular weight and dispersity

| Sample | $[\text{AA}]:[\text{Cu}^{2+}]$ ratio | M^n | $M_{\text{n, theo}}$ | D | Conversion (%) |
|-------------------------------|--------------------------------------|--------|----------------------|-----|----------------|
| Poly(n-butyl methacrylate) | | | | | |
| 1 ^a | 48:1 | 49,500 | 36,480 | 1.3 | 76 |
| 2 | 48:1 | 39,600 | 32,160 | 1.4 | 67 |
| 3 | 25:1 | 40,500 | 29,280 | 1.5 | 61 |
| 4 | 10:1 | 40,600 | 35,520 | 1.4 | 74 |
| 5 | 2:1 | 40,200 | 35,520 | 1.5 | 74 |
| Polystyrene | | | | | |
| 6 ^a | 48:1 | 40,000 | 29,920 | 1.3 | 85 |
| 7 | 48:1 | 37,800 | 32,032 | 1.2 | 91 |
| 8 | 25:1 | 41,700 | 32,384 | 1.3 | 92 |
| 9 | 10:1 | 38,900 | 31,680 | 1.3 | 90 |
| 10 | 2:1 | 29,200 | 32,032 | 1.4 | 91 |
| Poly(tert-butyl methacrylate) | | | | | |
| 11 ^a | 48:1 | 40,000 | 41,760 | 1.4 | 87 |
| 12 | 48:1 | 49,700 | 37,920 | 1.3 | 79 |
| 13 | 25:1 | 41,400 | 39,840 | 1.3 | 83 |
| 14 | 10:1 | 49,300 | 41,280 | 1.4 | 86 |
| 15 | 2:1 | 47,400 | 35,520 | 1.4 | 74 |

^a20 wt% acetone was added to the aqueous phase by keeping the total volume constant. [initiator]:[ligand]:[monomer] = 1:1.1:337.8, $T = 80^\circ\text{C}$, $t = 4$ h, $[\text{Cu}^{2+}] = 0.15 \mu\text{mol}/\text{ml}$, [Pluronic F-127] = 0.013 g/ml.

acetone to the aqueous phase. All polymers were characterized using, THF-GPC and DLS measurements of the emulsions.

Table 1 shows the effect of the $[\text{AA}]:[\text{Cu}^{2+}]$ ratio on the molar mass and dispersity of each of the monomers. For comparison, the polymerizations of nBMA, styrene,

and *t*BMA were also conducted with acetone in the aqueous phase and are labeled as sample 1^a, 6^a, and 11^a, respectively (see Table 1). For all polymers, dispersity remained similar with or without acetone. However, the resulting molar masses of PnBMA and PS were higher when acetone was included in the aqueous phase. All conditions were kept constant, including initiator and monomer concentrations; therefore, the increase of molar mass of PnBMA and PS in the acetone system is hypothesized to be due to improved transport of monomers to the growing polymer particles through the aqueous phase. Because the two monomers are the most hydrophobic in our studies, the incorporation of acetone helps transport monomers through the aqueous phase into the monomer phase at a faster rate, which would help increase molecular weights. When acetone is removed from the system, hydrophobic monomer diffusion from droplets to the polymer particles would be limited.

On the other hand, this trend was not observed for PtBMA and the molar mass increased when acetone was removed from the aqueous phase. The difference in these trends may be attributed to differences in solubility in the aqueous phases, i.e. their relative hydrophobicity, which can be compared via their partition coefficients, *logP*. The *t*BMA monomer is a much more hydrophilic monomer with a *logP* value of 1.86, compared to nBMA and styrene, whose *logP* values are 2.23 and 2.67, respectively. Therefore, the monomer can diffuse through the aqueous phase (without acetone) and can continue to propagate the polymerization more easily than styrene or nBMA. These differences are also apparent in their emulsion stability and will be discussed further.

The influence of AA concentration on each polymerization was also studied. The [AA]:[Cu²⁺] ratios were varied from a large [48]:[1] excess to a smaller [2]:[1] ratio, as seen in Table 1. The GPC traces of the resulting

polymers are shown in Figure 1. Reducing the amount of AA molar excess with respect to Cu²⁺ was found to have a small effect on molar mass and dispersity for each of the three monomers; for PS and PtBMA, [AA]:[Cu²⁺] ratios 10:1 and above result in narrow and consistent GPC traces. For PnBMA, curves remain consistent at all AA concentrations. It is hypothesized that the hydrophilic Cu¹⁺-Br/TPMA complex enters the particles at a slow, controlled rate, even at high concentrations of AA. This allows a low concentration of growing polymer chains within each particle, instead of an increasingly radical concentration from the excess AA.

Using excess AA during the polymerization is expected to jeopardize control over the polymerization since there must exist an appropriate balance between Cu²⁺ and Cu¹⁺ species. However, our results show that using a large excess of reducing agent still provides the same level of control over lower amounts. Since the system relies on TBAB to act as a shuttling agent for the catalyst,^{25,30,31} it is possible that the diffusion of Cu¹⁺-Br/TPMA is limited by the TBAB shuttle. Once Cu²⁺ is converted to Cu¹⁺, it becomes hydrophobic enough to prefer the monomer phase instead of the aqueous phase. However, the reduced complex likely sits at the water/particle interface and diffuses at a slow, reduced rate without jeopardizing the control over the polymerization.

Kinetic experiments of the three monomers with a concentration of 0.366 mol/L and a [AA]:[Cu²⁺] ratio of [48]:[1] were conducted with a [monomer]:[initiator ratio] of 337.8:1 (Table 1, sample 2, 7, 12). The first-order kinetic plots (Figure 2) shows a linear relation for the first 60 min of the polymerization. The *k*_{app} values were determined as 0.013 min⁻¹ for *t*BMA, 0.033 min⁻¹ for nBMA and 0.022 min⁻¹ for styrene, respectively. For all three monomers a first-order kinetic polymerization was observed indicating a constant number of propagating species until the beginning of termination after 60 min.

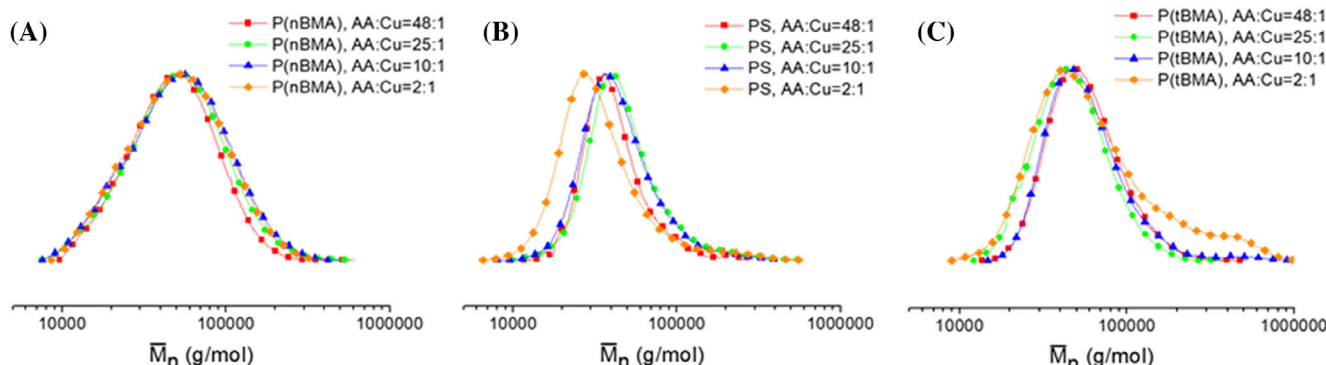


FIGURE 1 THF-GPC traces of (A) P(nBMA), samples 2–5 (B) PS, samples 7–10 (C) P(*t*BMA), samples 12–15; with different [AA]:[CuBr₂] ratios. [monomer] = 0.366 mol/L. [Pluronic F-127] = 0.08 g/ml. The AA solution feeding rate was constant over a period of 4 h at 20 μ l/min (4.8 ml total)

Whereas the rate of polymerization of nBMA and styrene are similar the rate of polymerization for *t*BMA is lower.

Dynamic light scattering (DLS) measurements of the post-synthesis reaction mixtures with varying amounts of AA were conducted in order to investigate the emulsion stability and are shown in Figure 3.

The size distributions of PS and PnBMA particles after polymerization measured by DLS suggest polymer particles have a diameter of around 40–60 nm, see Figure 3A,B. Additionally, particle size measurements were also conducted at various time intervals throughout the polymerization to show that both PS and PnBMA particles remain a consistent size throughout, see Figure S1A,B. The consistency in the DLS measurements taken during and after the polymerization for PS and PnBMA indicates that there is proper colloidal stability between the surfactant and monomers.

Although the polymer particle size distribution was similar between PS and PnBMA, the polymer dispersity

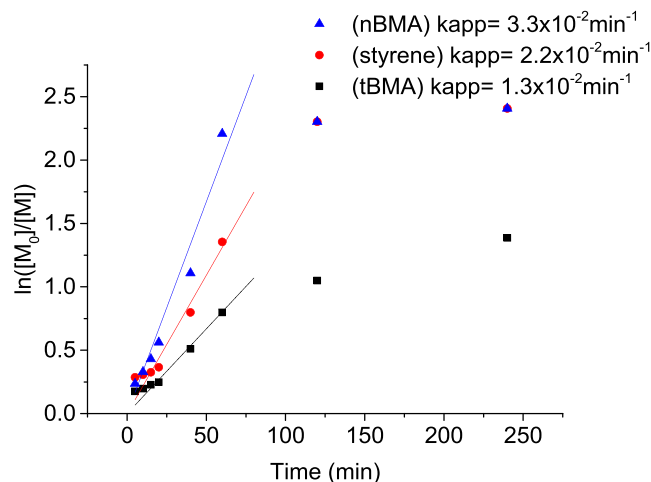


FIGURE 2 First-order kinetic plot of (Table 1, samples, 2, 7, 12); [AA]:[Cu²⁺] ratio of [48]:[1]. [Monomer] = 0.366 mol/L. [Pluronic F-127] = 0.08 g/ml. The AA solution feeding rate was constant over a period of 4 h at 20 $\mu\text{l}/\text{min}$ (4.8 ml total). Initiator concentration was 1 mM

between both polymers varied. Poly(styrene) consistently had a lower dispersity than PnBMA and is thought to be a result of differences in monomer hydrophobicity. Styrene has a logP value of 2.67, while nBMA's logP value is 2.23. Since styrene is more hydrophobic, it is hypothesized that monomer diffusion in and out of the droplets during the polymerization was reduced, therefore, resulting in the controlled growth of the polymer chain.³²

In contrast, the PtBMA emulsions post-polymerization show particles on the order of 40–60 nm as well as larger aggregates with sizes ranging up to several micrometers. As *t*BMA is the most hydrophilic monomer used in this work (log P = 1.86), its higher affinity for the aqueous phase compared to styrene and nBMA may lead to increased monomer migration into other particles and causing aggregation. Figure S1C, also gives evidence of colloidal instability at the end of the polymerization at the 40-min interval, whereas at the beginning of the PtBMA polymerization, a unimodal particle size distribution is observed at 40 nm. A small shoulder appears at \sim 100 nm and subsequent aliquots show a slow increase in size until the end of the polymerization, which likely continues after the reaction is terminated to yield the bimodal size distribution shown in Figure 3C. The bimodal particle size distribution is an indication of colloidal instability between the monomer and the surfactant which results in Ostwald ripening.^{33,34} It is worth noting that in the case of PtBMA, the addition of acetone to the aqueous phase resulted in no aggregation, suggesting increased emulsion stability (Figure S2).

The differences in particle size and stability are thought to be a function of monomer hydrophilicity and incompatibility with the surfactant employed. An increase in monomer diffusion in and out of the polymer particle is expected with more hydrophilic monomers, particularly when the aqueous phase does not include acetone. All polymer particles post-polymerization when 20 wt% acetone is included in the aqueous phase, including PtBMA, are unimodal and do not show signs of

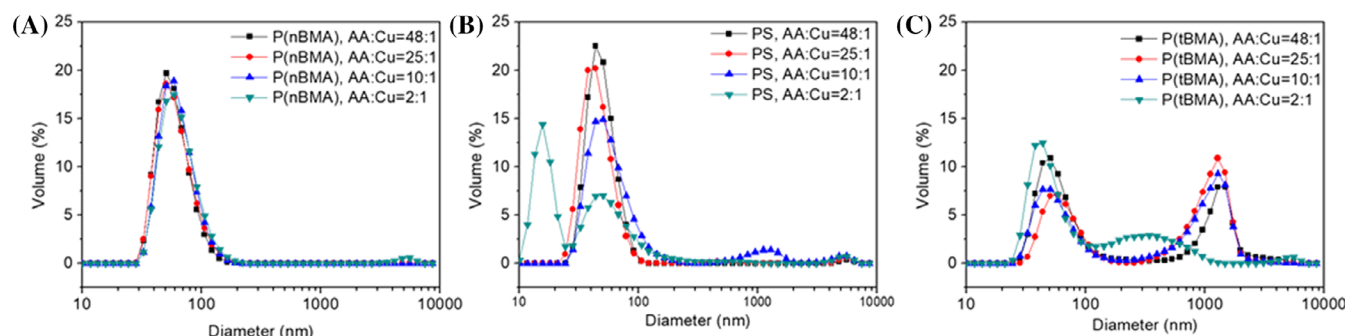


FIGURE 3 Emulsion size distributions of (A) P(nBMA), (B) PS, and (C) P(tBMA), with different [AA]:[Cu²⁺] ratios (Table 1, samples, 2–5; 7–10; 12–15). [Monomer] = 0.366 mol/L. [Pluronic F-127] = 0.08 g/ml. The AA solution feeding rate was constant over a period of 4 h at 20 $\mu\text{l}/\text{min}$ (4.8 ml total)

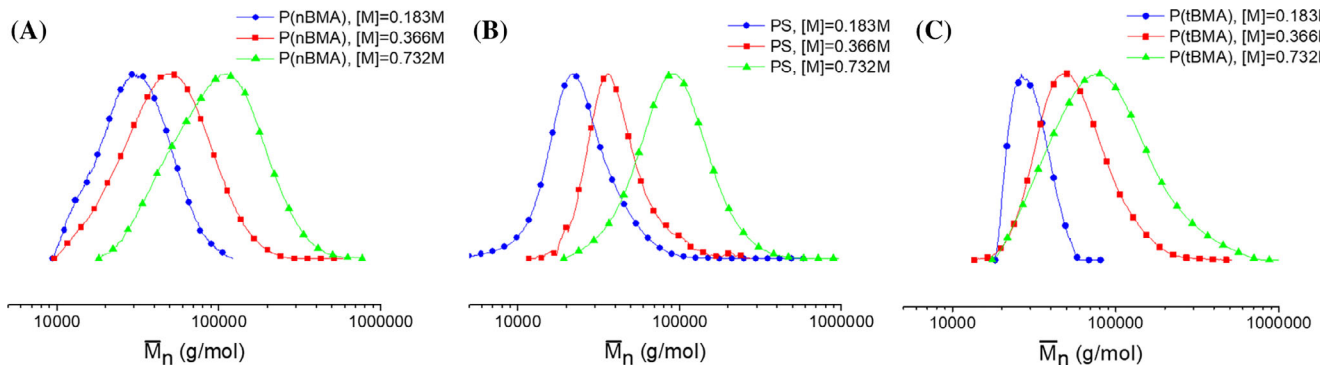


FIGURE 4 THF-GPC traces of (A) PnBMA, (B) PS, and (C) PtBMA with different monomer concentrations (Table 1, samples, 2–5; 7–10; 12–15). The [AA]:[Cu²⁺] ratio was [48]:[1] and [Pluronic F-127] = 0.08 g/ml. the AA solution feeding rate was constant over a period of 4 h at 20 μ l/min (4.8 ml total)

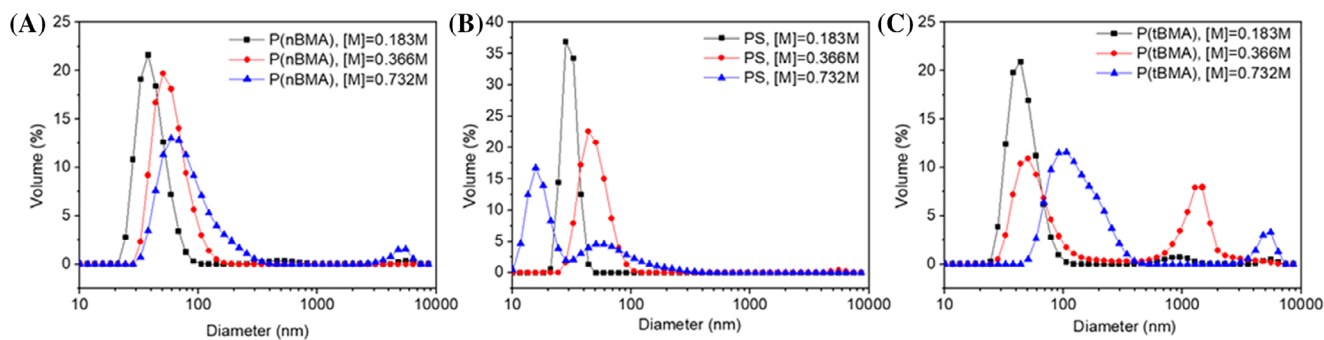


FIGURE 5 DLS measurements for samples with varying monomer concentrations Table S1: (A) PnBMA, samples 1–2; (B) PS, samples 3–4; (C) PtBMA, samples 5–6

aggregation (Figure S2). The unimodal particle size distributions indicate that acetone can help play a role in particle stability and reduce Ostwald ripening. Other studies have also described the use of hydrophobes as a way to control Ostwald ripening.^{33,34} However, in completely aqueous dispersed systems, our results suggest that Pluronic F-127 may not be compatible with hydrophilic monomers.

Polymers with different molar masses were synthesized with a [48]:[1] ratio of [AA]:[Cu²⁺] by varying the monomer concentrations. The GPC analyses for these polymers are shown in Figure 4, (additional data are compiled in Table S1).

For each monomer investigated, a low monomer concentration (0.183 mmol/ml) results in a low dispersity and an experimental molar mass close to its $M_{n,\text{theo}}$. Polymer particles also show high stability and an average size of 30 nm for all. However, while PS and PnBMA synthesis remained controlled for higher monomer concentrations (0.732 mmol/ml), there was a significant increase in dispersity for PtBMA (Table S1, entry 5). One potential reason for a decrease in reaction control could be due to increased monomer diffusion from one particle to another. Polymer particles for experiments with

monomer concentrations 0.366 and 0.732 M indicate that Ostwald ripening occurs in both instances. It is possible that with the development of a bimodal particle size distribution, as shown by DLS measurements (Figure 5C), each growing polymer chain will also have a distribution in the amount of monomer in the particle in which they are growing in, resulting in a broader molecular weight distribution. These results suggest that hydrophobic monomers can be polymerized by the miniemulsion ARGET ATRP system described in this work with a high level of polymerization control and colloidal stability. However, more hydrophilic monomers, like *t*BMA, may need to be polymerized either at low enough monomer concentrations to avoid bimodal particle size distributions, or employ methods which would allow for better colloidal stability between the monomer and surfactant.

3 | CONCLUSION

Miniemulsion polymerizations were carried out using ARGET ATRP to form poly(n-butyl methacrylate), poly-styrene, and poly(tert-butyl methacrylate) with low dispersity and without the support of organic solvents

acting as phase transfer agents. The influence of the monomer hydrophobicity on the polymerization system under various polymerization conditions was evaluated. It was determined that monomer hydrophobicity does not have a large influence on molecular weight distribution, as all monomers provided good polymerization control with dispersities between 1.2 and 1.4. The ratio between reducing agent, ascorbic acid and catalyst also had a small effect on molecular weight and dispersity, as it was found that $[AA]:[Cu^{2+}]$ ratios above [10]:[1] can be employed without jeopardizing control of the polymerization. However, at low ratios of $[AA]:[Cu^{2+}]$, for example, [2]:[1], the molecular weight distributions tend to broaden for all polymers.

Although high degrees of control over molecular weight and dispersity were achieved, in the case of *t*BMA, the most hydrophilic monomer, bimodal polymer particle distributions were measured by DLS at all $[AA]:[Cu^{2+}]$ ratios. The reduction in colloidal stability suggests that the non-ionic Pluronic F-127 surfactant is less effective in stabilization of PtBMA droplets and results in Ostwald ripening. Decreasing the monomer concentration to 0.183 mmol/ml results in unimodal polymer particle size distribution, with low molecular weight dispersity and an experimental molar mass close to its $M_{n,\text{theo}}$. On the other hand, increasing monomer concentrations (0.732 mmol/ml) broadened polymer dispersity and resulted in bimodal polymer particle size distributions. For PnBMA and PS, dispersities were unchanged and polymer particles remained unimodal. These results suggest that for this miniemulsion ARGET ATRP system, hydrophilic monomers like *t*BMA can be polymerized in a controlled manner but their colloidal stability with the non-ionic surfactant must be considered.

4 | EXPERIMENTAL SECTION / METHODS

4.1 | Materials

Stabilized styrene (99%), L-ascorbic acid, tetrabutylammonium bromide (99%), and copper (II) bromide (99%, extra pure, anhydrous) were all purchased from Acros Organics and used as received. *N*-butyl methacrylate, *N*-tert-butyl methacrylate, tris(2-pyridyl methyl) amine (TPMA, >98%), ethyl 2-bromo-3-butynoate (EBIB), Pluronic F-127 were purchased from TCI and used as received.

4.2 | Instrumentation

Molar mass and dispersity (D) were determined via an Agilent 1100 gel permeation chromatography (GPC)

system with a differential refractive index detector, using tetrahydrofuran (THF) as eluent. This system employed a pre-column (SDV; particle size 3 μm , dimension 8.0 mm \times 50 mm), followed by two identical PSS SDV columns (particle size 3 μm , dimension 8.0 mm \times 300 mm, 1000 \AA) and a third PSS SDV column with a larger pore size (particle size 3 μm , dimension 8.0 mm \times 300 mm, 10,000 \AA). Narrow-dispersity polystyrene standards were used to calibrate the system. The flow rate was 1.0 ml/min. The software PSS WinGPC 6 was used to determine the molar mass and dispersity of the measured samples.

DLS measurements of droplet size and emulsion stability in water were performed using a Malvern Zetasizer Nano ZS90.

4.3 | Polymer synthesis

The following synthesis for sample 1 in Table 1 is representative of the other syntheses in this paper. TBAB (1.934 g, 6 mmol), CuBr₂ (2 mg, 8.96 μmol), and tris (2-pyridylmethyl) amine (TPMA) (20.80 mg, 71.63 μmol) were added to water (45.2 ml) in a three-neck 100-ml round-bottom flask equipped with a stir bar. In a separate vial, the monomer (styrene, 1.62 g, 15.54 mmol) and initiator (EBiB, 12.6 mg, 0.065 mmol) were added to 10 ml of an aqueous Pluronic F-127 solution (0.08 g/ml). The solution was vortexed and sonicated until a milky white emulsion was formed. The monomer-containing solution was then added to the 100-ml round-bottom flask, forming a cloudy white emulsion and sonicated for 10 more minutes. The flask was sealed with a septum and the solution was purged with argon for 30 min. An argon-filled balloon equipped with a needle was then attached to the septum. Finally, in a separate vial, a solution of ascorbic acid (18 mM, 5 ml) was prepared and purged with argon for 30 min before being fed to the reaction using a syringe pump at a rate of 20 $\mu\text{l}/\text{min}$ (4.8 ml for 4 h) at 80°C. The polymerization was stopped after 4 h by opening the reaction to air and adding methanol to precipitate the polymer. The polymer was then centrifuged, dissolved in THF, and precipitated again in methanol. Finally, the polymer was collected and washed with water before drying under a vacuum at 60°C. For GPC analysis, the purified polymer was dissolved in THF at 1 mg/ml.

ACKNOWLEDGMENTS

The authors would like to extend their gratitude to the Air Force Office of Scientific Research (AFOSR FA9550-17-1-0038), and also to the Air Force Research Laboratory for prior support. Alicia Cintora would like

to acknowledge the National Science Foundation for an NSF Graduate Research Fellowship (DGE-1650441). This work made use of the Cornell Center for Materials Research Shared Facilities, which is supported through the NSF MRSEC Program (DMR-1719875). DLS measurements were made using facilities provided by the Cornell Energy Systems Institute (CESI).

ORCID

Florian Käfer  <https://orcid.org/0000-0003-4988-3812>

Christopher K. Ober  <https://orcid.org/0000-0002-3805-3314>

REFERENCES

- [1] V. J. Cunningham, A. M. Alswieleh, K. L. Thompson, M. Williams, G. J. Leggett, S. P. Armes, O. M. Musa, *Macromolecules* **2014**, 47(16), 5613.
- [2] H. De Brouwer, J. G. Tsavalas, F. J. Schork, M. J. Monteiro, *Macromolecules* **2000**, 33(25), 9239.
- [3] E. Groison, S. Brusseau, F. D'Agosto, S. Magnet, R. Inoubli, L. Couvreur, B. Charleux, *ACS Macro Lett.* **2012**, 1(1), 47.
- [4] B. Charleux, J. Nicolas, *Polymer* **2007**, 48, 5813.
- [5] M. E. Thomson, A. M. Manley, J. S. Ness, S. C. Schmidt, M. F. Cunningham, *Macromolecules* **2010**, 43, 7958.
- [6] Y. Kagawa, M. Kawasaki, P. B. Zetterlund, H. Minami, M. Okubo, *Macromol. Rapid Commun.* **2007**, 28, 2354.
- [7] Y. Kagawa, P. B. Zetterlund, H. Minami, M. Okubo, *Macromolecules* **2007**, 40, 3062.
- [8] K. E. Min, L. I. Mei, K. Matyjaszewski, *J. Polym. Sci. Part A Polym. Chem.* **2005**, 43(16), 3616.
- [9] J. Qiu, S. G. Gaynor, K. Matyjaszewski, *Macromolecules* **1999**, 32, 2872.
- [10] R. W. Simms, M. F. Cunningham, *Macromolecules* **2007**, 40, 860.
- [11] R. W. Simms, M. F. Cunningham, *J. Polym. Sci. Part A Polym. Chem.* **2006**, 44, 1628.
- [12] R. W. Simms, M. F. Cunningham, *Macromol. Symp.* **2008**, 261, 32.
- [13] M. Li, K. Matyjaszewski, *Macromolecules* **2003**, 36, 6028.
- [14] M. Li, K. Min, K. Matyjaszewski, *Macromolecules* **2004**, 37, 2106.
- [15] H. Peng, S. Cheng, L. Feng, *Polym. Int.* **2004**, 53, 828.
- [16] W. Li, K. Min, K. Matyjaszewski, F. Stoffelbach, B. Charleux, *Macromolecules* **2008**, 41, 6387.
- [17] K. Min, H. Gao, K. Matyjaszewski, *J. Am. Chem. Soc.* **2006**, 128, 521.
- [18] K. Min, H. Gao, K. Matyjaszewski, *J. Am. Chem. Soc.* **2005**, 127, 3825.
- [19] Y. Kitayama, M. Yorizane, Y. Kagawa, H. Minami, P. B. Zetterlund, M. Okubo, *Polymer* **2009**, 50, 3182.
- [20] J. K. Oh, F. Perineau, B. Charleux, K. Matyjaszewski, *J. Polym. Sci. Part A Polym. Chem.* **2009**, 47, 1771.
- [21] F. Stoffelbach, B. Belardi, J. M. R. C. A. Santos, L. Tessier, K. Matyjaszewski, B. Charleux, *Macromolecules* **2007**, 40, 8813.
- [22] K. Min, J. Kwon Oh, K. Matyjaszewski, *J. Polym. Sci. Part A Polym. Chem.* **2007**, 45, 1413.
- [23] Y. Wang, F. Lorandi, M. Fantin, P. Chmielarz, A. A. Isse, A. Gennaro, K. Matyjaszewski, *Macromolecules* **2017**, 50, 8417.
- [24] A. M. Elsen, J. Burdyńska, S. Park, K. Matyjaszewski, *ACS Macro Lett.* **2013**, 2, 822.
- [25] R. Cordero, A. Jawaid, M.-S. Hsiao, Z. Lequeux, R. A. Vaia, C. K. Ober, *ACS Macro Lett.* **2018**, 7, 459.
- [26] R. Razeghi, F. Kazemi, N. Nikfarjam, Y. Shariati, B. Kaboudin, *Eur. Polym. J.* **2021**, 144, 110195.
- [27] B. P. Fors, C. J. Hawker, *Angew. Chem. Int. Ed.* **2012**, 51, 8850.
- [28] A. Anastasaki, V. Nikolaou, Q. Zhang, J. Burns, S. R. Samanta, C. Waldron, A. J. Haddleton, R. McHale, D. Fox, V. Percec, P. Wilson, D. M. Haddleton, *J. Am. Chem. Soc.* **2014**, 136, 1141.
- [29] N. J. Treat, H. Sprafke, J. W. Kramer, P. G. Clark, B. E. Barton, J. Read de Alaniz, B. P. Fors, C. J. Hawker, *J. Am. Chem. Soc.* **2014**, 136, 6096.
- [30] G. M. Miyake, J. C. Theriot, *Macromolecules* **2014**, 47, 8255.
- [31] D. Y. Wu, F. Käfer, N. Diaco, C. K. Ober, *J. Polym. Sci. A* **2020**, 58, 2310.
- [32] A. Simakova, S. E. Averick, D. Konkolewicz, K. Matyjaszewski, *Macromolecules* **2012**, 45, 6371.
- [33] W. I. Higuchi, J. Misra, *J. Pharm. Sci.* **1962**, 51, 459.
- [34] A. S. Kabal'nov, A. V. Pertzov, E. D. Shchukin, *Colloids Surf.* **1987**, 24, 19.

SUPPORTING INFORMATION

Additional supporting information may be found in the online version of the article at the publisher's website.

How to cite this article: A. Cintora, F. Käfer, C. Yuan, C. K. Ober, *J. Polym. Sci.* **2021**, 1. <https://doi.org/10.1002/pol.20210658>